A Novel Approach to Synthesis of Non-uniform Conformal Reflectarray Antennas

M. Karimipour and A. Pirhadi

Faculty of Electrical and Computer Engineering
Shahid Beheshti University G.C (SBU),Tehran, +98, Iran
M.Karimipour@mail.sbu.ac.ir, a_pirhadi@sbu.ac.ir

Abstract ─ This paper presents an accurate method to synthesize a shaped-beam conformal reflectarray (RA) antenna based on the phase synthesis of its equivalent aperture. For this purpose particle swarm optimization (PSO) is used to determine the optimal phase distribution on the reflective surface of the antenna. Furthermore, a method based on meshing the aperture of the antenna has been adopted to evaluate its radiation fields. By dividing the equivalent aperture of the antenna into small parts, the induced current in each part is approximated appropriately.Then the radiation fields can be evaluated via the sum of simple integrals. This approach provides a direct correlation between the amplitude and the phase of reflection coefficient of the RA elements with the radiation fields of the antenna. Therefore, the effect of elements can be considered directly in the optimization process. Another advantage of this method is that it can be used to synthesize non-flat RA antennas. Furthermore, in the proposed method the effects of the angle, polarization, amplitude, and phase of the radiated fields from the feed antenna are fully considered in the synthesis procedure. To verify the proposed method a shaped beam parabolic RA antenna in the X-band has been synthesized. The simulation results represent a good agreement with the simulation results obtained from the commercial full-wave electromagnetic (EM) software, CST microwave studio.

Index Terms - Optimization process, reflectarrays, radiation fields, and shaped-beam antenna.

I. INTRODUCTION

Antennas with shaped beam radiation patterns are required in many communication systems such as satellite communications, radar, and wireless communications. Reflector antennas and array antennas are among the most frequently used antenna types for these purposes. In most of the reflector antennas, the shaped radiation pattern is obtained by shaping the surface of the reflector, which makes it difficult to fabricate [1]. In array antennas, making the shaped radiation pattern is done by suitable excitation of the array elements that needs a complex feeding network [2].

The shaped radiation pattern can also be obtained using RA antennas. The RA antenna is a combination of reflector and array antennas. It consists of a reflective surface including the radiation elements and a feed, which is located in a certain distance from the reflective surface [3]. In printed RA antennas the radiation elements are designed using printed structures such as printed microstrip patches, dipoles, rings, split rings [3], etc. One important feature of the RA antennas is their ability to produce an arbitrary radiation pattern by creating the appropriate EM field distribution on their aperture. This is done by suitable embedding of the radiation elements on the reflective surface [4]. Unlike shaped beam reflector antennas and array antennas, it is not necessary to shape the reflective surface or design the complex feeding network. In these antennas the radiation elements are used to create the shaped radiation pattern by tuning their corresponding reflection phases. Based on this property the RA antennas can also be used to design a multi-beam radiation pattern, electronically scanned radiation pattern [4, 5], etc.

Submitted On: Feb. 24, 2013
Accepted On: Oct. 9, 2013

The first steps for designing a shaped beam RA antenna is obtaining the amplitude and phase distributions of the EM fields on the reflective surface or equivalent aperture based on the desired radiation pattern. The second step is designing the radiation elements according to the extracted EM field distributions in the first step. To realize the first step, radiated far fields must be calculated based on EM characteristics of the reflective surface (including the magnitude and the phase of the tangential fields), afterward the EM characteristics of the reflective surface must be adjusted using a suitable iterative process in order to shape the radiation pattern. Different methods have been used for this purpose. The most important method is the array concept method. In this method, the conventional array theory is used to calculate the far field radiation pattern from the RA elements [6-10]. Other method is the equivalent aperture field method based on the physical optic (PO) approximation. The array concept method is simple and fast but the feed antenna effect is not considered in this analysis method. The equivalent aperture method is more accurate than the array concept method and takes the feed antenna into account in the analysis procedure.

The amplitude of the EM field components on the reflective surface or the equivalent aperture of the RA antenna is directly determined from the radiated field of the feed. Therefore, only the phase of the field components on the reflective surface or equivalent aperture can be used to shape the radiation pattern of the RA antenna. For this reason, most of the synthesis methods of RA antennas are carried out to approximate or optimize the phase distribution on the surface of the RA antennas. It must be noticed that the direct optimization process, in which all the element dimensions are simultaneously optimized in an iterative process to obtain the required radiation pattern, is computationally unaffordable because of the large number of elements [11].

Alternating projection method also known as intersection approach [12] is one of the most widely used methods to synthesize RA antennas [13-15]. This approach is significantly useful for large RA antennas synthesis because of the reduced computational time for convergence. In some cases, especially in non-symmetric designs, this optimization procedure is trapped in local minima and cannot satisfy the goal function [15]. Therefore it is necessary to use an optimization algorithm based on the local and global searches to solve this problem.

In the second step, after determining the optimum phase distribution of the fields on the aperture of RA antennas, appropriate elements must be designed to provide this phase distribution. The main challenges in this step are designing the radiation elements as phase shifters with a linear phase characteristic, low sensitivity with respect to the incident angle and a wide operating frequency bandwidth (in order to improve the bandwidth of RA [16]). Microstrip patches with the same dimensions and variable stubs [3], patches with variable sizes [9] and variable rotation angles [17], rings with or without a split [18, 19] and using the same elements in an irregular grid [20] are some of the structures that have been used so far.

In this paper in the first step an accurate analysis method is developed to obtain the radiated far fields of the RA antenna from the tangential fields on its surface based on the PO approximation. To evaluate the radiation integrals, which describe the relation between the amplitude and phase of the tangential fields on the surface of the RA and the radiation fields, a procedure based on meshing the equivalent aperture of the reflective surface has been adopted [21]. In principle, this method has been used to analyze reflector antennas and is developed to analyze and synthesize RA antennas in this paper. The most advantageous feature of this method is that it can be implemented on non-flat surfaces. In this method the equivalent aperture of the reflective surface is divided into some meshes and the amplitude and phase of the tangential electric fields in each mesh are approximated by linear functions. For evaluating the radiation fields accurately, especially in the side lobe regions, the mesh density must be 1 to 3 meshes per wavelength. Based on this analysis method and using PSO algorithm, the optimum phase distribution of the tangential fields on the RA surface is determined for shaping the radiation field patterns. In each mesh the amplitude of the tangential electric fields on the reflective surface is also obtained from the full-wave modeling of the feed antenna. In this analysis method, by considering the position of the radiation elements

with respect to the feed, the effects of the polarization and the incident angle are taken into account in the design process, which leads to an increase in the accuracy of the synthesis method. After obtaining the optimum phase distribution of the tangential fields on the reflective surface, phase distribution is implemented using appropriate radiation elements. These elements are constructed of a combination of square patches and rings. In order to verify the suggested design procedure, a conformal RA antenna with a cosecant squared radiation pattern in the elevation plane and a pencil beam radiation pattern in the azimuth plane, has been designed and simulated in the X-band. Results from the optimization procedure indicate a good agreement with the simulation results obtained from the full-wave commercial software (CST microwave studio [22]).

In section II the basic design equations for the analysis of RA antennas for a general curved surface are presented. In section III, a conformal RA is synthesized based on the method in section II and PSO algorithm. Section IV presents the full-wave simulation results of the optimized structure.

II. THE BASIC DESIGN EQUATIONS FOR REFLECTARRAY ANTENNAS

The general configuration of the RA antenna with an arbitrary cross section and a curved surface is shown in Fig. 1.

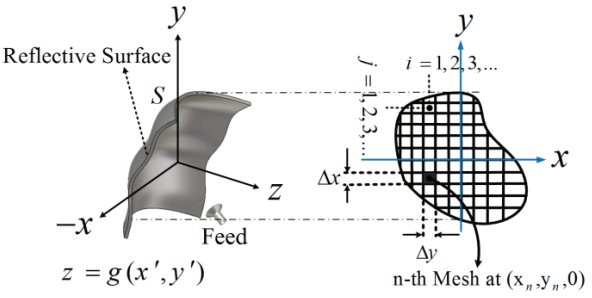

Fig. 1. Geometry of the RA antenna.

The analysis method should be in a way that it can be used for non-flat reflective surfaces. Based on the PO approximation of the radiated far field from a surface with an arbitrary curvature, the electric radiation field is calculated as [23],

$$\bar{E} = -j\beta\frac{e^{-j\beta r}}{2\pi r}\hat{r}\times\iint_{s}\hat{n}\times\bar{E}_a e^{j\bar{k}\cdot\bar{r}'}ds \tag{1}$$

where $\hat{n}\times\bar{E}_a$ is the tangential electric field on the radiating surface and $\hat{n} = n_x\hat{x} + n_y\hat{y} + n_z\hat{z}$ is the normal vector at any point of the radiating surface. The radiating surface curvature is demonstrated as $z = g(x, y)$. Therefore, the radiation integral in equation (1) can be expressed as,

$$\bar{E} = -j\beta\frac{e^{-j\beta r}}{2\pi r}\hat{r}\times \iint_{s'}\sqrt{1+(\frac{\partial g}{\partial x'})^2+(\frac{\partial g}{\partial y'})^2}\,\hat{n}\times\bar{E}_a e^{j\bar{k}\cdot\bar{r}'}ds' \tag{2}$$

where s' is the projection of the reflective curvature on the XY plane. By expanding equation (2) the radiated far field components are,

$$E_x^{ff} = -j\beta\frac{e^{-j\beta r}}{2\pi r}\iint_{s'}\Big[(n_x E_{ay} - n_y E_{ax})(\sin\theta\sin\phi) - (n_z E_{ax} - n_x E_{az})\cos\theta\Big]\times\sqrt{1+(\frac{\partial g}{\partial x'})^2+(\frac{\partial g}{\partial y'})^2}\times e^{jk_0[x'\sin\theta\cos\phi+y'\sin\theta\sin\phi+g(x',y')\cos\theta]}ds' \tag{3a}$$

$$E_y^{ff} = -j\beta\frac{e^{-j\beta r}}{2\pi r}\iint_{s'}\Big[(n_y E_{az} - n_z E_{ay})\cos\theta - (n_x E_{ay} - n_y E_{ax})(\sin\theta\cos\phi)\Big]\times\sqrt{1+(\frac{\partial g}{\partial x'})^2+(\frac{\partial g}{\partial y'})^2}\times e^{jk_0[x'\sin\theta\cos\phi+y'\sin\theta\sin\phi+g(x',y')\cos\theta]}ds' \tag{3b}$$

$$E_z^{ff} = -j\beta\frac{e^{-j\beta r}}{2\pi r}\iint_{s'}\Big[(n_z E_{ax} - n_x E_{az})\sin\theta\cos\phi - (n_y E_{az} - n_z E_{ay})(\sin\theta\sin\phi)\Big]\times\sqrt{1+(\frac{\partial g}{\partial x'})^2+(\frac{\partial g}{\partial y'})^2}\times e^{jk_0[x'\sin\theta\cos\phi+y'\sin\theta\sin\phi+g(x',y')\cos\theta]}ds'. \tag{3c}$$

For an arbitrary surface, solving the radiation integrals of equation (3a-3c) is complicated and time consuming. To reduce the complexity and solve the radiation integrals in equation (3), the equivalent aperture is divided into small sub-sections (based on the proposed method in [21]). Then in general form, the integrands of equations (3a-3c) are approximated as sum of linear functions with unknown coefficients as,

$$A = \sum_{i=1}^{N}\sum_{j=1}^{M}\int_{x_i}^{x_{i+1}}\int_{y_j}^{y_{j+1}} a_{P\_ij}\times e^{j\left[\alpha_{P\_ij}+\beta_{P\_ij}(x'-x_i)+\gamma_{P\_ij}(y'-y_j)\right]}\times(a_2x'+b_2y'+c_2)\times e^{jk_0[x'\sin\theta\cos\phi+y'\sin\theta\sin\phi+(a_1x'+b_1y'+c_1)\cos\theta)]}ds'. \tag{4}$$

The integrand in equation (4) consists of three parts. The first part $a_{P\_ij} \times e^{j\left[\alpha_{P\_ij}+\beta_{P\_ij}(x'-x_i)+\gamma_{P\_ij}(y'-y_j)\right]}$, which is the approximation of the tangential electric field in each sub-section on the equivalent aperture. The subscript (*ij*) denotes the position of the sub-sections and the subscript (*p*) denotes the electric field components. The unknown coefficients α_{y_ij}, β_{y_ij} and γ_{y_ij} are used to represent the phase distribution of the tangential fields in each sub-section. These coefficients are adjusted to produce the desired radiation pattern. Therefore, this analysis procedure is only based on the phase synthesis of the aperture. The second part, approximates $\sqrt{1+(\frac{\partial g}{\partial x'})^2+(\frac{\partial g}{\partial y'})^2} \times n_P(x',y',z')$ with a linear function as ($a_2x'+b_2y'+c_2$) and finally, in the third part, the function g(x', y') is approximated with ($a_1x'+b_1y'+c_1$) in each sub-section. The coefficients a_1, b_1, c_1, a_2, b_2, and c_2 are determined based on linear approximations of the corresponding functions in each sub-section. Therefore, the radiation integrals in equation (3) can be expressed as the sum of simple integrals with exponential integrands that can be solved easily in the closed forms. The smaller sub-sections, lead to the more accurate radiation fields. Calculations show that a good accuracy is obtained for sub-sections with dimensions of about λ/2 or smaller.

In most analyses of the RA antennas, the radiation fields from the feed antenna are approximated by a cosine function ($\cos^q$) [6, 8, 13]. In this approximation, the effect of the phase center of the feed and its cross-polarization component are not considered. In our analysis, to solve these problems the radiated fields from the horn antenna are obtained using the full-wave EM simulator. In this case the a_{p_ij} coefficients in equation (4) are replaced by the amplitude of the radiated fields from the feed at each sub-section of the RA surface.

III. SYNTHESIS OF SHAPED-BEAM CONFORMAL REFLECTARRAY ANTENNAS

In the previous section it was shown how we can obtain the radiation fields from the aperture by approximating the tangential fields on it. In this section, based on this analysis method, a shaped beam conformal RA antenna, which is designed at 10 GHz, is synthesized.

A. Antenna configuration and radiated fields formulation

The geometry of the antenna is shown in Fig. 2. As shown in this figure a non-flat surface with a parabolic cross section is considered as the reflective surface in which the curve function is $g(x',y')=\frac{x'^2}{4a}-b$. where a=10cm and b=0.06cm.

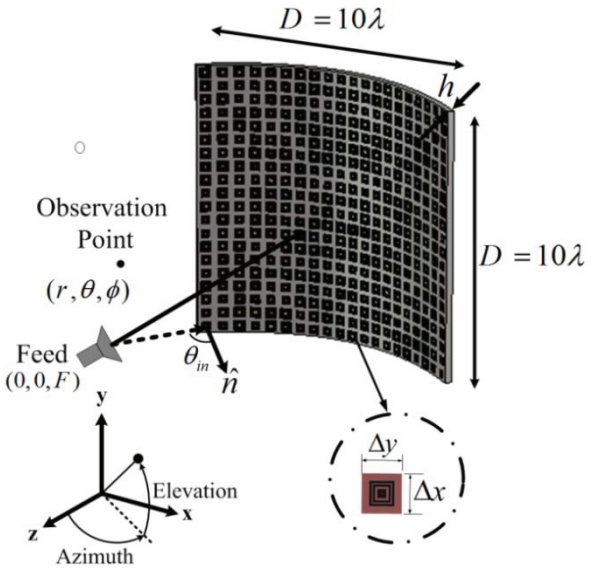

Fig. 2. Geometry of the proposed conformal RA antenna.

The radiation elements are placed on the reflective surface to provide the suitable phase distribution in order to generate the desired radiation pattern. A conical horn antenna is used as the feed, which has 40° and 45°, 3 dB beam-widths in E- and H-Planes, respectively. The feed antenna is designed to produce a vertical polarization. The vertical polarization is considered as the co-Polarization component of the radiation fields. Therefore, E_y^{ff} is used in the elevation and the azimuth planes to construct the radiation patterns. Based on equations (3b) and (4), the co-Polarization electric field can be written as

$$E_{co\_pol}^{ff} = j\beta\frac{e^{-j\beta r}}{2\pi r}\left[\sin\theta\cos\phi A_1+\cos\theta A_2\right], \qquad (5)$$

where A_1 and A_2 are

$$A_1 = \sum_{i=1}^{N}\sum_{j=1}^{M} a_{y\_ij} \times e^{j\left[\alpha_{y\_ij} - \beta_{y\_ij} x_i - \gamma_{y\_ij} y_j - k_0 b \cos\theta\right]} \times I_1 I_2, \quad (6a)$$

$$A_2 = \sum_{i=1}^{N}\sum_{j=1}^{M} a_{y\_ij} \times e^{j\left[\alpha_{y\_ij} - \beta_{y\_ij} x_i - \gamma_{y\_ij} y_j - k_0 b \cos\theta\right]} \times I_2 I_3, \quad (6b)$$

and I_1, I_2, and I_3 are as follows,

$$I_1 = \int_{x_i}^{x_{i+1}} \frac{-x'}{2a} e^{j[(k_0 \sin\theta\cos\phi + \beta_{y\_ij})x' + a_1(x' - x_i) + b_1]} dx', \quad (7a)$$

$$I_2 = \int_{y_j}^{y_{j+1}} e^{j[k_0 \sin\theta\sin\phi + \gamma_{y\_ij}]y'} dy', \quad (7b)$$

$$I_3 = \int_{x_i}^{x_{i+1}} e^{j[(k_0 \sin\theta\cos\phi + \beta_{y\_ij})x' + a_1(x' - x_i) + b_1]} dx' \quad . \quad (7c)$$

In which a_1 and b_1 are,

$$a_1 = \frac{y_{i+1} - y_i}{x_{i+1} - x_i} = \frac{k_0 \cos\theta}{4a}\left(\frac{x_{i+1}^2 - x_i^2}{\Delta x}\right) \quad (8a)$$

$$b_1 = \frac{k_0 \cos\theta}{4a} x_i^2. \quad (8b)$$

In the optimization procedure, the phase coefficients of all sub-sections (α_{y_ij}, β_{y_ij}, and γ_{y_ij}) are considered as the inputs of the optimization algorithm and the desired radiation pattern is considered as the goal function. In this study, the goal function is a shaped beam with a cosecant squared form in the elevation plane and a pencil beam in the azimuth plane. The optimization procedure to determine the unknown coefficients is described in the following section based on the PSO algorithm.

B.Using the PSO algorithm for optimizing the structure

As is stated in the previous section, an intelligent evolutionary algorithm called PSO is used to adjust the phase coefficients of the approximation function of the tangential fields of the reflective surface. In this method, local and global search methods are combined to achieve the optimal results. In the PSO algorithm, particles move in a multi dimensional search space. During this movement, every particle adjusts its position with respect to adjacent particles while considering their prior experience. In general the position of each particle at each stage is expressed as follows [24],

$$\bar{v}_k(t) = \bar{v}_k(t-1) + c_1 r_1 \times [\bar{P}_k(t-1) - \bar{k}(t-1)] + c_2 r_2 \times [\bar{G}_k(t-1) - \bar{k}(t-1)] \quad (9)$$

$$\bar{k}(t) = \bar{k}(t-1) + \bar{v}_k(t) \quad .$$

In equation (9) $\bar{k}$ and $\bar{v}$ represent the position and the velocity of coefficients (α_{y_ij}, β_{y_ij}, and γ_{y_ij}), respectively. The positive constant c_1 and c_2 are usually $c_1 = c_2 = 2$. The best previous position (the position giving the best fitness value) of the k-th particle (coefficient) is presented as $\bar{P}_k(t-1)$ and $\bar{G}_k(t-1)$ denotes the best k-th particle among all the particles in the group. Also, r_1 and r_2 are two random values in the range (0, 1). Equation (9) is used to update the velocity of the coefficients as a function of their previous velocity, the previous position, k (t-1), the best experienced (position) personal, P_k (t-1), and the best experienced group, G_k (t-1). Afterward, the coefficients move toward a new position. These coefficients are used to calculate the radiation fields of the antenna in each step. In the next step, the error function or the fitness function is defined as the absolute difference between the target and the calculated radiation fields. The optimization procedure is continued until the error function converges to the acceptable value.

Optimal radiation patterns or mask functions are represented in Fig. 3 for the elevation and azimuth planes. The mask functions are a cosecant squared pattern in the elevation plane with a 35° coverage region and a pencil beam pattern in the azimuth plane with a 5° coverage region. Moreover, the side lobe levels in the elevation and azimuth planes are -20dB and -30dB, respectively.

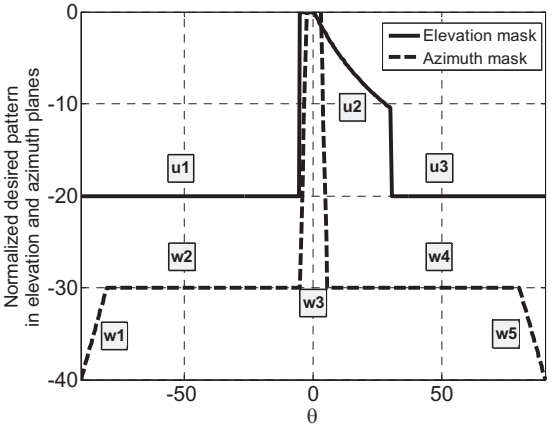

Fig. 3. Desired radiation patterns in the elevation and azimuth planes.

The Error function by assuming $w_1 = w_5$ and $w_2 = w_4$ is defined as follows,

$$\begin{aligned}\text{Fitness function} = 2\Bigg[& w_3 \sum_{\theta=0}^{5} \left|F_A - F_{Desired}\right| + \\ & w_4 \sum_{\theta=5}^{80} \left|F_A - F_{Desired}\right| + w_5 \sum_{\theta=80}^{90} \left|F_A - F_{Desired}\right| \Bigg] \\ & + \Bigg[u_1 \sum_{\theta=-90}^{-5} \left|F_E - F_{Desired}\right| + u_2 \sum_{\theta=-5}^{30} \left|F_E - F_{Desired}\right| \\ & + u_3 \sum_{\theta=30}^{90} \left|F_E - F_{Desired}\right| \Bigg],\end{aligned} \tag{10}$$

where F_A and F_E are the calculated radiation patterns in the azimuth and elevation planes and $F_{Desired}$ is the desired radiation pattern in each step of the PSO. According to Fig. 3 the assigned weights are shown by u and w for each region in the radiation patterns. Given the importance of the radiation pattern in the shaped region in the azimuth and elevation planes, higher weights are assigned to form the radiation patterns.

C. Synthesis results using the PSO algorithm

In this section synthesis results using the PSO algorithm are presented. For this purpose, the area of each cell is considered by about $\lambda/2 \times \lambda/2 \times \lambda/2$, which leads to 400 sub-sections, as shown in Fig. 2. The feed antenna is located at (0, 0, 233 mm) in which the maximum incident angle to the reflector is about 30^o. The PSO input parameters to start the optimization procedure are assumed as, $(\alpha_{ij}, \beta_{ij}, \gamma_{ij}) \in [-11,11]$, $(V_{\alpha_{ij}}, V_{\beta_{ij}}, V_{\gamma_{ij}}) \in 0.2 \times [-11,11]$, $u_1 = 3.9$, $u_2 = 8.2$, $u_3 = 4.9$, $w_3 = 8.2$, $w_4 = 5.9$, and $w_5 = 3$. The number of particles is 100 and the number of iterations is 3000. Figure 4 shows the optimized phase distribution of the tangential electric fields obtained by the PSO algorithm on the RA surface. The produced phase distribution on the RA surface from the radiated fields of the feed antenna is transformed to the optimal phase distribution by the RA elements. Considering the optimal phase distribution, co-polarization and cross-polarization components of the radiated far fields are shown in Fig. 5. As is shown in Fig. 5 there is a good agreement between the optimized radiation patterns and the desired patterns. The convergence of the fitness function with respect to the iteration steps is shown in Fig. 6.

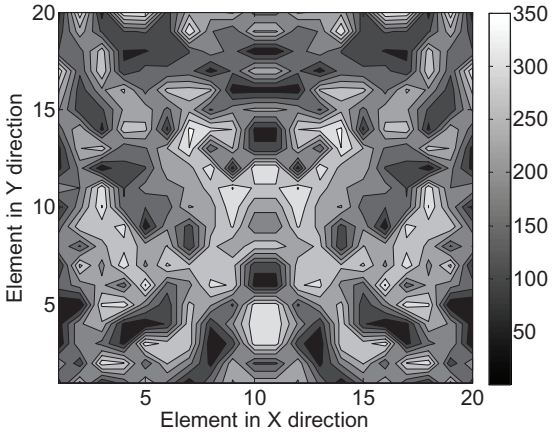

Fig. 4. The optimal phase distribution (in degrees) obtained from the PSO on the RA surface.

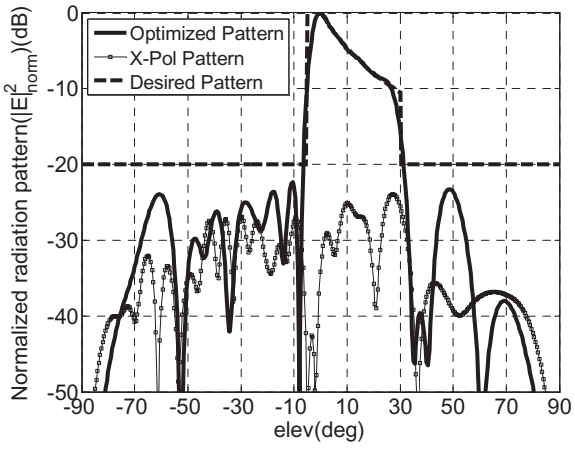

(a)

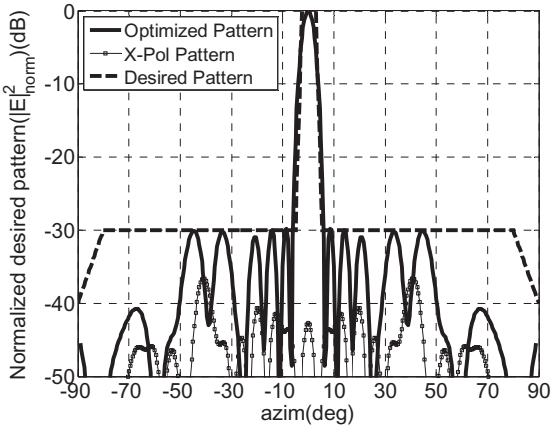

(b)

Fig. 5. Optimized radiation patterns (a) elevation plane and (b) azimuth plane.

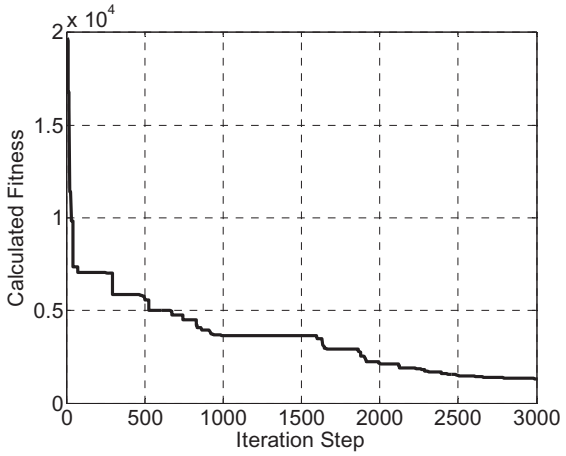

Fig. 6. The convergence of the fitness function with respect to the iteration steps.

D. Designing the elements to obtain the optimum phase distribution

Knowing the phase of the radiated fields from the feed antenna on the sub-sections of the RA surface, $\phi_{Incident}$ and the optimal phase distribution from the PSO, $\phi_{Desired}$, the phase for the elements $\phi_{Element}$, can be determined as,

$$\phi_{Element}(i,j)=\phi_{Desired}(i,j)-\phi_{Incident}(i,j) \quad . \qquad (11)$$

Different types of radiation elements have been used to provide the required phase [3, 25]. In this paper a single layer square patch and rings are used as the RA elements [26]. The geometry of a single cell of this structure is shown in Fig. 7. The reflection phase coefficient of this structure is stable for relatively large incident angles. Therefore, study of normal incident angles is sufficient to obtain the reflection phase properties. The HFSS software using the Floquet's port and periodic boundary conditions concept is used to simulate the reflection phase coefficient of a single cell. The simulation results have been depicted in Fig. 7 for the incident plane wave with horizontal polarization and various incident angles. The substrate of the structure is a type of foam with ε_r = 1.006, $\tan\delta$ = 0, L = 1.5 cm, and t = 7 mm.

In each sub-section, the dimensions of elements are determined in a way that they realize the optimal phase distribution. To this end the parametric study shows that w = 0.125 L_2, L_1/L_2 = 0.5, and L_3 = 3w + L_2 can provide our required reflection phase coefficients. Because of the wide variety of the optimum phase distributions on the RA surface, it is necessary to design the radiation elements with different dimensions in each sub-section on the RA, which is a time consuming process. In this paper, in order to simplify this procedure a neural network is used. This network is trained so that the reflection phase coefficients and incident angles are considered as the inputs and the dimensions of the elements are considered as the outputs of the network. After training the network, based on the optimum phase distribution on the RA, the dimensions of suitable element in each subsection is determined quickly.

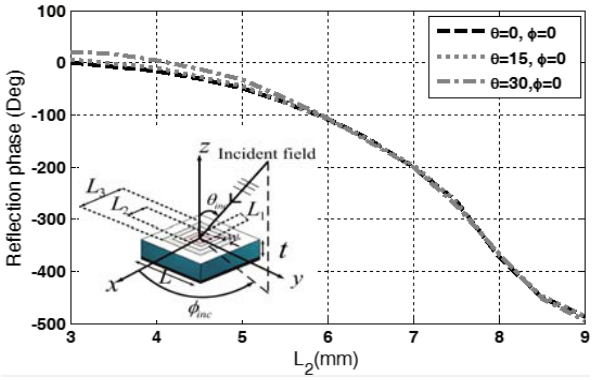

Fig. 7. Reflection phase coefficient of the proposed element at 10 GHz.

IV. SIMULATION RESULTS

To validate the proposed synthesis method, the dimensions of the elements are extracted by neural networks and located in their place on the reflective surface. Then the whole structure is simulated by the full-wave electromagnetic simulator, CST software, using the integral equation solving method. The normalized electric radiation field patterns of the antenna for the elevation and azimuth planes are represented in Fig. 8. As can be seen in this figure, the desired radiation patterns have been well realized in the elevation and azimuth planes.

One of the most advantageous features of the conformal RA antenna in comparison with the flat type is its wider bandwidth [8]. In order to show this, the radiation patterns of the synthesized conformal RA antenna in the previous section and a flat RA antenna with the same aperture size are studied for a given frequency band. As shown in Figs. 9 and 10, both of the conformal and flat RA antennas are synthesized in the 10 GHz frequency and show a good agreement with the desired radiation patterns in the azimuth and elevation

planes. Study of these structures in the lower and upper operating frequencies indicates that the conformal RA has a more stable behavior compared with the flat one. This means that the conformal RA antenna, regardless of its elements, has a wider frequency bandwidth in comparison with the flat one.

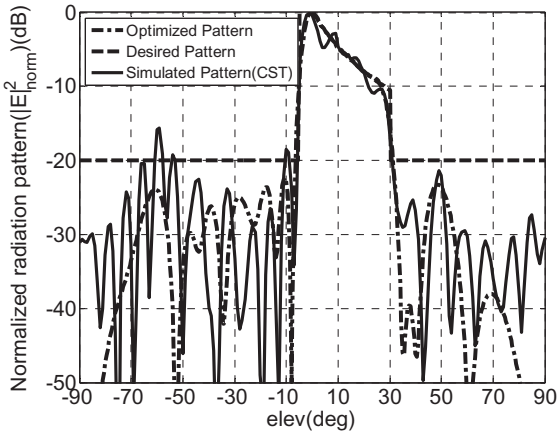

Fig. 8. The optimized pattern in Matlab and the simulated pattern in CST (a) elevation plane and (b) azimuth plane.

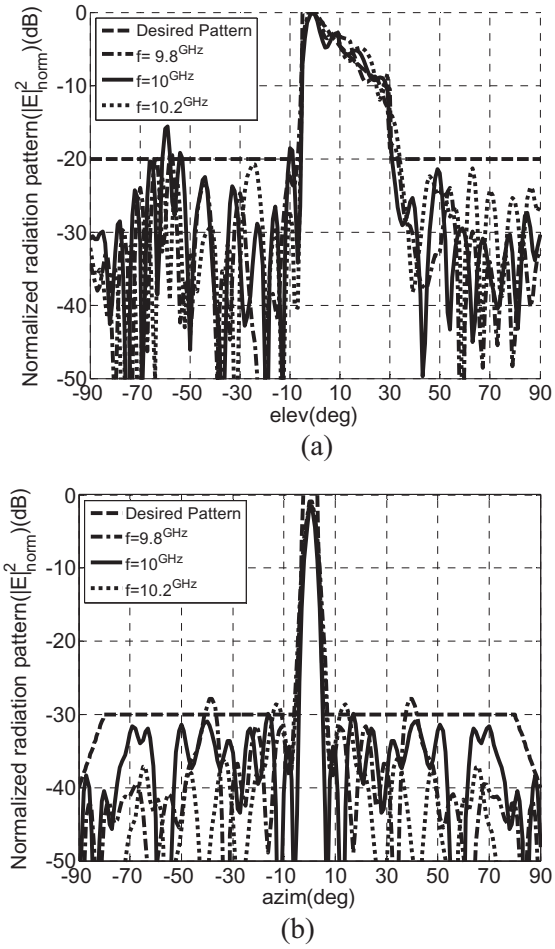

Fig. 9. Simulated radiation patterns of the conformal RA antenna for different frequencies (a) elevation plane and (b) azimuth plane.

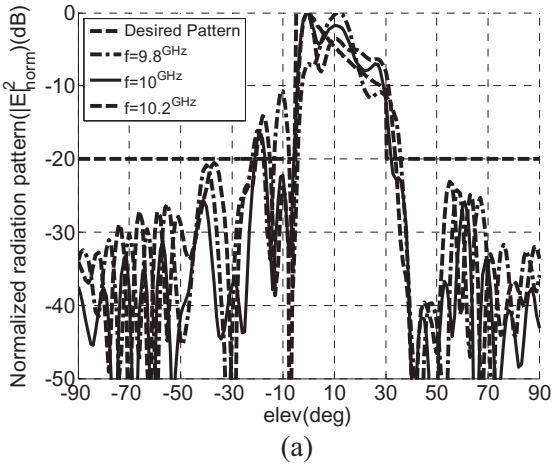

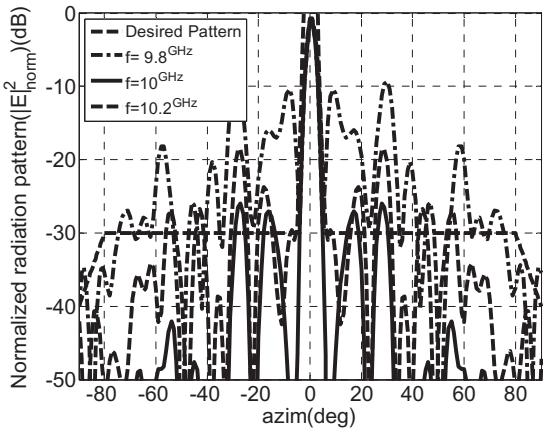

(b)

Fig. 10. Simulated radiation patterns of the flat RA antenna for different frequencies (a) elevation plane and (b) azimuth plane.

V. CONCLUSION

A method with the PSO algorithm was used to synthesize a shaped beam conformal RA antenna. The capability of the proposed method to synthesize the conformal structures has been evaluated by synthesis of a parabolic RA antenna. Employing this technique shows significant improvement in analyzing the non-flat RA antennas. It was shown that there is a good agreement between the desired and simulated radiation patterns, especially in the shaped beam regions. Moreover, it was shown that the conformal RA antennain comparison with the flat one has a wider operating bandwidth.

ACKNOWLEDGMENT

The authors would like to thank the Iran Telecom Research Center (ITRC) for the support of this research.

REFERENCE

[1] J. Bergmann, R. Brown, P. Clarricoats, and H. Zhou, "Synthesis of shaped-beam reflector antenna patterns," *Microwaves, Antennas and Propagation, IEE Proceedings H*, vol. 38, pp. 48-53, 1988.

[2] T. Ismail and Z. Hamici, "Array pattern synthesis using digital phase control by quantized particle swarm optimization," *IEEE Trans. Antennas Propagat*., vol. 58, no. 6, June 2010.

[3] J. Huang and J. Encinar, *Reflectarray Antennas*, IEEE Press, John Wiley & Sons, Inc., Hoboken, New Jersey, 2007.

[4] P. Nayeri, F. Yang, and A. Elsherbini, "Design and experiment of a single-feed quad-beam reflectarray antenna," *IEEE Trans. Antennas Propagat*., vol. 60, no. 2, pp. 1166-1171, Feb. 2012.

[5] S. Hum, M. Okoniewski, and R. Davies, "Realizing an electronically tunable reflectarray using varactor diode-tuned elements," *IEEE Microwave and Wireless Components Letters*, vol. 15, no. 6, pp. 422-424, June 2005.

[6] E. Almajali, D. McNamara, J. Shaker, and M. Chaharmir, "Derivation and validation of the basic design equations for symmetric sub- reflectarrays," *IEEE Trans. Antennas Propagat.*, vol. 60, no. 5, pp. 2336-2346, Feb. 2012.

[7] A. Trastoy, F. Ares, and E. Moreno, "Phase-only synthesis of non-φ-symmetric patterns for reflectarray antennas with circular boundary," *IEEE Antennas and Wireless Propag ation Letters*, vol. 3, pp. 246-248, 2004.

[8] G. Zhao and Y. Jiao, "Design of broadband dual-polarization contoured-beam reflectarray for space applications," *28th Annual Review of Progress in Applied Computational Electromagnetics (ACES)*, pp. 790-794, Columbus, Ohio, April 2012.

[9] D. Pozar and T. Metzler, "Analysis of a reflectarray antenna using microstrip patches of variable size," *Electronics Letters*, vol. 29, no. 8, pp. 657-658, Apr. 1993.

[10] J. Encinar, "Design of two-layer printed reflectarrays using patches of variable size," *IEEE Trans. Antennas Propagat*., vol. 49, no. 10, pp. 1403-1410, Oct. 2001.

[11] J. Encinar, M. Arrebola, L. de la Fuente, and G. Toso, "A transmit-receive reflectarray antenna for direct broadcast satellite applications," *IEEE Trans. Antennas Propagat*., vol. 59, no. 9, pp. 3255-3264, Sep. 2011.

[12] O. Bucci, G. Franceschetti, G. Mazzarella, and G. Panariello, "Intersection approach to array pattern synthesis," *IEE Proceedings*, vol. 137, no. 6, pp. 349-357, Dec. 1990.

[13] P. Nayeri, A. Elsherbeni, and F. Yang, "Design, full-wave simulation, and near-field diagnostics of reflectarray antennas using FEKO electromagnetic software," *28th Annual Review of Progress in Applied Computational Electromagnetics (ACES)*, pp. 503-508, Columbus, Ohio, Apr. 2012.

[14] J. Zornoza, R. Leberer, J. Encinar, and W. Menzel, "Folded multilayer microstrip reflectarray with shaped pattern," *IEEE Trans. Antennas Propagat*., pp. 510-518, vol. 54, no. 2, Feb. 2006.

[15] J. Encinar and J. Zornoza, "Three-layer printed reflectarrays for contoured beam space applications," *IEEE Trans. Antennas Propagat*., vol. 52, no. 5, pp. 1138-1148, May 2004.

[16] J. Encinar and J. Zornoza, "Broadband design of three-layer printed reflectarrays," *IEEE Trans. Antennas Propagat*., vol. 51, no. 7, pp. 1662-1664, July 2003.

[17] J. Huang and R. Pogorzelski, "A Ka-band microstrip Reflectarray with elements having variable rotation angles," *IEEE Trans. Antennas Propagat*., vol. 46, pp. 650-656, May 1998.

[18] Y. Li, M. Biakowski, K. Sayidmarie, and N. Shuley, "Single-layer microstrip reflectarray with double elliptical ring elements for bandwidth enhancement," *Microwave and Optical Technology Letters*, vol. 53, no. 5, May 2011.

[19] S. Yusop, N. Misran, M. Islam, and M. Ismail, "Design of high performance dual frequency concentric split ring square element for broadband reflectarray antenna," *Applied Computational Electromagnetics Society (ACES)* Journal, vol. 27, no. 4, pp. 334-339, Apr. 2012.

[20] M. Zhou, S. Sorensen, P. Meincke, E. Jorgensen, O. Kim, O. Breinbjerg, and G. Toso, " Design and analysis of printed reflectarrays with irregularly positioned array elements," *European Conference on Antennas and Propagation*, pp. 1619-1623, 2011.

[21] C. Scott, *Modern Method of Reflector Antenna Analysis and Design*, Artech House, 1990.

[22] CST, (Computer Simulation Technology), Microwave Studio 2011, Integral-Equation Simulation Tool.

[23] C. Balanis, *Antenna Theory Analysis and Design*, 3rd ed., John Wiley & Sons, Inc., Hoboken, New Jersey 2005.

[24] Y. Shi and R. Eberhart, "Empirical study of particle swarm optimization," *Proceedings of the 1999 Congress on Evolutionary Computation*, pp. 1945-1 950, 1999.

[25] M. Maddahali and K. Forooraghi, "Design of broadband single layer printed reflectarray using Giuseppe Peano fractal ring," *Applied Computational Electromagnetics Society (ACES) Journal*, vol. 28, no. 2, pp. 150-155, Feb. 2013.

[26] Q. Li, Y. Jiao, and G. Zhao, "A novel microstrip rectangular-patch/ring-combination reflectarray element and its application," *IEEE Antennas and Wireless Propagation Letters*, vol. 8, pp. 1119-1122, 2009.

Majid Karimipour received his B.S. and M.S. degrees in Electrical Engineering 2008 and 2011 from Shahrekord University, Shahrekord, Iran and Shahid Beheshti University (SBU), Tehran, Iran, Respectively. His major research interests are the development and design of reflectarray antennas for wireless communications, evolutionary algorithms, and shaped beam antennas synthesis.

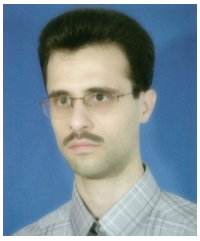

Abbas Pirhadi received B.S. degree in Electrical Engineering from the Isfahan University of Technology, Isfahan, Iran 2000, and M. S. and Ph.D. degree in Communication Engineering from Tarbiat Modares University (TMU), Tehran, Iran in 2002 and 2007, respectively. From 2002 to 2006, he joined the Antenna and Propagation Group of the Iran Telecommunication Research Center (ITRC) as a researcher. Also, in 2008 he joined the Shahid Beheshti University (SBU) where he is the Assistant Professor at the faculty of Electrical and Computer engineering. His research interests include microwave antennas, theoretical and computational electromagnetic with applications to antenna theory and design.